# Laser-induced band gap collapse in GaAs

Y. Siegal, E. Glezer, L. Huang and E. Mazur

*Department of Physics and Division of Applied Sciences, Harvard University, Cambridge, MA 02138*

## ABSTRACT

We present recent time-resolved measurements of the linear dielectric constant of GaAs at 2.2 eV and 4.4 eV following femtosecond laser pulse excitation. In sharp contrast to predictions based on the widely-used Drude model, the data show an interband absorption peak coming into resonance first with the 4.4-eV probe photon energy and then with the 2.2-eV probe photon energy, indicating major changes in the band structure. The time scale for these changes ranges from within 100 fs to a few picoseconds, depending on the incident pump pulse fluence.

## 1. INTRODUCTION

The field of laser-induced structural change in semiconductors has generated considerable interest since the discovery of laser annealing in the 1970's.[1] This interest originally centered on whether the underlying mechanism for the induced changes is a thermal melting process or a nonthermal destabilization of the covalent bonds. The thermal model assumes that the free charge carriers (electrons and holes) excited by the laser pulse quickly transfer energy to the lattice through phonon emission, allowing the lattice to heat up quickly to the melting temperature and melt. The nonthermal or plasma model assumes slower electron-lattice energy transfer and asserts that the excitation of a critical density of electrons from bonding valence states to antibonding conduction states will directly destabilize the lattice structure.[2]

Early experimental work in this field involving excitation pulse widths on the order of 30 ps or longer demonstrated that the excitation causes strong, rapid lattice heating and agreed with computer simulations based on the thermal model. Later work using Raman spectroscopy showed that the electron-lattice energy relaxation time is on the order of a few picoseconds,[3] supporting the assumption in the thermal model of fast energy transfer between free carriers and the lattice. The development of femtosecond lasers renewed interest in this topic by opening up the possibility of depositing a large amount of energy in a semiconductor on a time scale which is short compared to the electron-lattice energy relaxation time. Because the excited free carriers are not equilibrated with the lattice on subpicosecond time scales, one might expect very different behavior in semiconductors irradiated by femtosecond excitation pulses.

A number of recent femtosecond pump-probe experiments suggest that the response of a semiconductor to intense femtosecond laser pulse excitation is indeed qualitatively different from the response to picosecond and nanosecond laser pulse excitation.[4-7] These experiments show the behavior of both linear



0-8194-1437-9/94/$6.00

reflectivity and second-harmonic generation in reflection of Si[4] or GaAs[5-7] as a function of pump-probe time delay. The results exhibit a sharp rise in the linear reflectivity as well as a vanishing of the second-harmonic signal within a few hundred femtoseconds of the excitation, long before significant heating of the lattice can take place.

However, interpretation of these linear reflectivity and second-harmonic generation results is difficult because they do not directly yield the behavior of intrinsic material properties. In particular, the linear reflectivity at a particular wavelength depends on both the real and imaginary parts of the dielectric constant at that wavelength. Furthermore, the measured second-harmonic radiation depends on the dielectric constant at both the fundamental and second-harmonic wavelengths as well as on the second-order susceptibility. The amount of information in the linear reflectivity and second-harmonic generation measurements, therefore, is not sufficient to uniquely determine the behavior of the linear or nonlinear optical material properties.

Without direct determination of the time-evolution of the dielectric constant, interpretation of previous reflectivity and second-harmonic data has relied on making assumptions about the form of the dielectric constant. Specifically, analysis of reflectivity data in picosecond and femtosecond laser-induced disordering experiments has been simplified by assuming that the changes to the dielectric constant induced by the excitation are dominated by the free carrier contribution to the optical susceptibility.[7-9] We can separate the dielectric constant into an interband transition term and a free carrier term:

$$\varepsilon(\omega) = 1 + 4\pi[\chi(\omega)_{\text{interband}} + \chi(\omega)_{\text{Drude}}], \tag{1}$$

with $\chi(\omega)_{\text{interband}}$ the contribution from interband transitions. The free carrier contribution to the dielectric constant is generally written as a Drude term,[9,10]

$$\chi(\omega)_{\text{Drude}} = \frac{Ne^2\tau^2}{m^*(1+\omega^2\tau^2)}\left[-1 + i\,\frac{1}{\omega\tau}\right], \tag{2}$$

where $\omega$ is the angular frequency of the incident light, $m^*$ is a reduced effective mass for the free carriers, $\tau$ is the average mean free time between collisions of free carriers with ions, and $N$ is the excited free carrier density. If under laser excitation the magnitude of the Drude term is larger than the change in $\chi(\omega)_{\text{interband}}$, one would expect the real part of the dielectric constant $\text{Re}(\varepsilon)$ to decrease linearly with excited free carrier density and therefore decrease monotonically with the fluence of the excitation pulse. Furthermore, for semiconductors, $\omega\tau >> 1$ in the visible, so according to this model the imaginary part of the dielectric constant $\text{Im}(\varepsilon)$ should increase with fluence only slightly .

To avoid relying on a model for the dielectric constant in interpreting femtosecond pump-probe experiments on GaAs, we directly determined the time evolution of the real and imaginary parts of the dielectric constant at photon energies of 2.2 eV and 4.4 eV following excitation with an intense, 70-fs pump pulse at 1.9 eV. At each probe frequency we measured the *p*-polarized reflectivity

at two different angles of incidence using two simultaneous 70-fs probe beams to obtain two independent measured quantities. We then converted each measured pair of reflectivities to the real and imaginary parts of the dielectric constant as a function of pump-probe time delay. We verified that our two-angle technique yielded dielectric constant values consistent with reflectivity measurements at a third angle of incidence. The data we present in this paper show that for excitation fluences on the order of 1 $kJ/m^2$, the Drude term described above is not a valid description of the induced changes to the dielectric constant. Our results indicate that the interband transition contribution to the optical susceptibility dominates the behavior of the dielectric constant, and not the free carrier contribution as has been generally assumed. This conclusion suggests that the reflectivity rise seen in a number of femtosecond experiments on semiconductors[4-8] is due to dramatic changes in the electronic band structure resulting from the excitation.

## 2. EXPERIMENTAL SETUP

### 2.1 Two-color amplified femtosecond laser system

The results presented in this paper involve measurements made using a two-color pump-probe technique. For one set of measurements we used a 70-fs, 1.9-eV pump beam and a simultaneous pair of 70-fs, 2.2-eV probe beams while for the other set of measurements we kept the same pump beam conditions but doubled the probe frequency to 4.4 eV. To generate pump and probe beams at different frequencies, we pass the amplified output of a colliding pulse modelocked laser through a 2-cm, single-mode, polarization-preserving optical fiber.[11] Self-phase modulation in the fiber broadens the spectrum of the input pulse from 5 nm to 200 nm. By splitting this continuum beam with a broad band beamsplitter, we can independently amplify different spectral regions within this 200-nm band width using two separate amplifier chains. A three-stage amplifier using the dye DCM produces a 300-$\mu$J pump beam centered at 635 nm with a 20-nm band width; a two-stage amplifier using the dye Rhodamine 6G produces a 30-$\mu$J probe beam centered at 570 nm with a 10-nm band width. Both amplifiers are pumped by a frequency-doubled, 10-Hz Nd:YAG laser. Following amplification, each beam is compressed by a separate grating pair to about a 70-fs pulse width (FWHM).

### 2.2 Time-resolved determination of the dielectric constant

To determine both the real and imaginary parts of the dielectric constant of GaAs with femtosecond time resolution, we simultaneously measure the reflectivity at two different angles of incidence as a function of pump-probe time delay. In the 2.2-eV experiment, the pair of probe beams is produced simply by splitting the 570-nm beam in two; In the 4.4-eV experiment, we first double the 570-nm beam in a 100-$\mu$m thick BBO crystal before splitting the beam. In both cases, the incident beams are polarized in the plane of incidence and are focused to the same spot on the sample, which is an insulating (110) GaAs wafer (Cr doped, $\rho > 7\times10^7$ W cm) in air. To monitor a uniformly excited region, we focus the probe

beams more tightly than the pump beam: the probed surface area is about 16 times smaller than the 0.01-$mm^2$ focal area of the pump beam on the sample. Uniform excitation in the probed region is further assured by the smaller penetration depth of the probe beams ($\leq$ 170 nm at 2.2 eV depending on the strength of the excitation and much smaller at 4.4 eV) compared to that of the pump beam (270 nm). The pump pulse fluence at each pump-probe time delay spans a range from 0 to 2.5 kJ/$m^2$. The probe beam fluence never exceeds 0.1 kJ/$m^2$ so as not to produce any detectable changes in the dielectric constant to within our experimental resolution. To avoid cumulative damage effects, we translate the sample during data collection so that each data point is obtained at a new spot on the sample.

We convert each pair of reflectivity measurements to the corresponding real and imaginary parts of the dielectric constant by numerically inverting the Fresnel formula for reflectivity as a function of incident angle. Setting one of the probe beam angles of incidence to the Brewster angle provides good sensitivity in distinguishing changes in Re($\varepsilon$) from changes in Im($\varepsilon$) because the *p*-polarized reflectivity at this angle is determined mainly by Im($\varepsilon$).[12] We base our choice of the second incident angle, which is not as critical, on constraints in the experimental setup. The two angles of incidence for the 2.2-eV measurements were 75.8° and 70.9° while in the 4.4-eV measurements we used 76.0° and 58.5°. To keep the angular separation between pump and probes small, we used a 63° incident angle for the pump beam in the 2.2-eV experiment and a 68° incident angle in the 4.4-eV experiment.

Because GaAs in air has an oxide layer on the surface, we use a three-phase model (air-oxide-GaAs) in converting the reflectivity measurements to dielectric constant. Surface roughness effects can also be accounted for in this type of model with the proper oxide layer effective thickness.[13] We calibrate the effective thickness of the oxide layer by measuring reflectivity as a function of incident angle in the absence of pump pulse excitation. Using the known dielectric constant of GaAs[14] and a value of $\varepsilon = 4$ for the dielectric constant of the oxide layer,[13] we fit the three-phase model to the measured angle dependence with the effective oxide layer thickness as a fit parameter. This procedure consistently yields an effective thickness of about 40 Å. In the 2.2-eV experiment the obtained value was 42 ± 4 Å while in the 4.4-eV experiment the value was 44 ± 4 Å.

As a consistency check for our determination of the dielectric constant, we measure the time-evolution of the reflectivity at a third angle of incidence under similar pump pulse excitation conditions at both probe frequencies. We then calculate the expected reflectivity at that third incident angle using our experimentally determined values for the dielectric constant. The calculated reflectivity showed good agreement with the measured reflectivity at a third angle of incidence for both the 2.2-eV and 4.4-eV data.

## 3. EXPERIMENTAL RESULTS

### 3.1 Dielectric constant at 2.2 eV

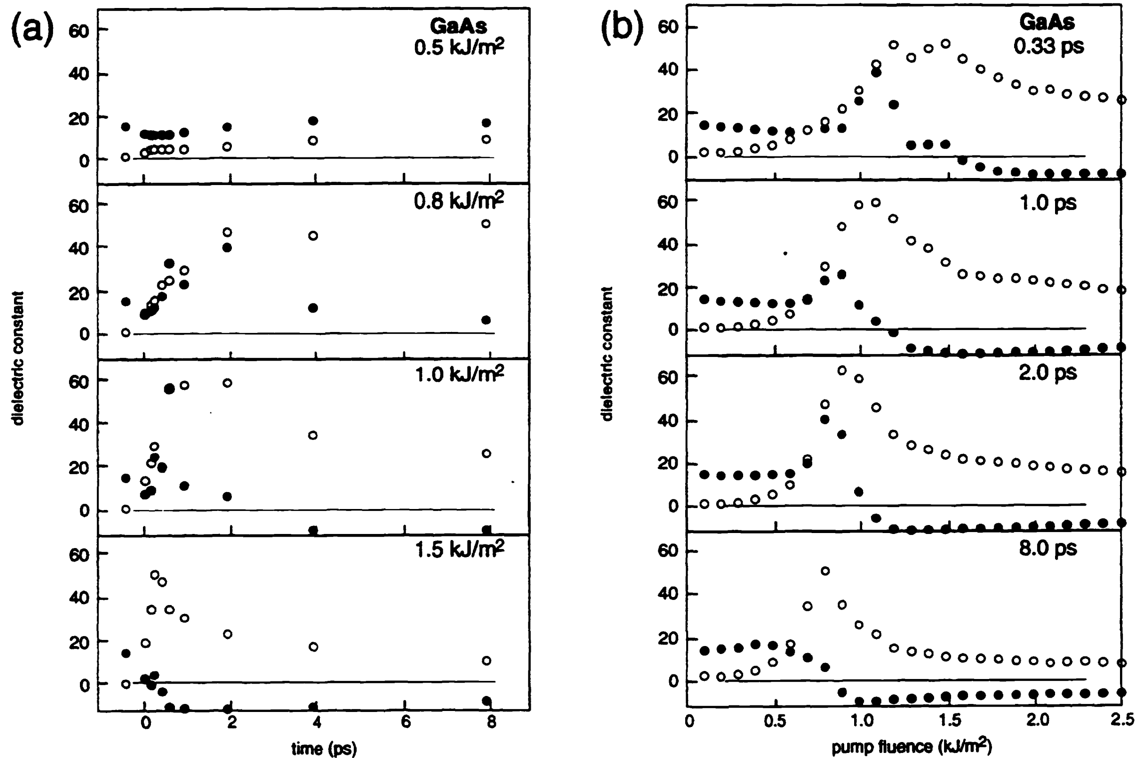


Fig. 1 a) Dielectric constant at 2.2 eV vs. pump-probe time delay for four different pump fluences. b) Dielectric constant at 2.2 eV vs. pump fluence for four different pump-probe time delays. ●: Re(ε), ○: Im (ε).

Figure 1 summarizes the experimental data on the dielectric constant at 2.2 eV. In Fig. 1a, the real (filled circles) and imaginary (open circles) parts of the dielectric constant are plotted vs. pump-probe time delay for four different excitation fluences; in Fig. 1b, the dielectric constant is plotted vs. pump fluence at four different time delays. As these plots clearly show, the change induced in the dielectric constant by the pump pulse excitation is completely different from that expected from the free carrier contribution to the optical susceptibility. At pump fluences near 1 $kJ/m^2$, Im(ε) starts at an initial value of about 2, rises to a peak near 60, and then drops to somewhere between 10 and 15 — a strong contrast to the slight, smooth increase predicted by the Drude model. Re(ε), meanwhile, initially decreases slightly but then increases before dropping sharply through zero. Note that the zero-crossing of Re(ε) coincides with the peak in Im(ε).

The results in Fig. 1 indicate that a strong interband absorption peak comes into resonance with the probe frequency as a result of the excitation. This resonance behavior is most striking in Fig. 1b, where the features are particularly sharp. Because the zero-crossing in Re(ε) is accompanied by a peak in Im(ε) rather than

by a steady increase, the resonance must result from an interband absorption peak and not from a free carrier plasma resonance. From the behavior of Re($\varepsilon$) both in time and as a function of pump fluence, we can infer the behavior of this interband absorption peak. For an absorption peak, Re($\varepsilon$) is positive at frequencies below the resonant frequency and negative at frequencies above the resonant frequency. Thus, the resonant frequency of the absorption peak evident in the data must start out above the probe frequency and then sweep down through it as a result of the excitation.

The rate at which this resonant frequency drops through the probe frequency depends on the strength of the excitation: the higher the pump fluence, the faster Re($\varepsilon$) drops through zero. Figure 2 illustrates this dependence by showing the time delay at which Re($\varepsilon$) crosses through zero plotted vs. pump fluence. For fluences around 2.0 kJ/m$^2$, the absorption peak comes into resonance with the probe frequency within a few hundred femtoseconds; at fluences just above 0.8 kJ/m$^2$, on the other hand, the absorption peak takes several picoseconds to come into resonance. For fluences below 0.8 kJ/m$^2$, Re($\varepsilon$) never goes through zero, indicating that the excitation is not strong enough to bring the resonant frequency of the peak down to the probe frequency.

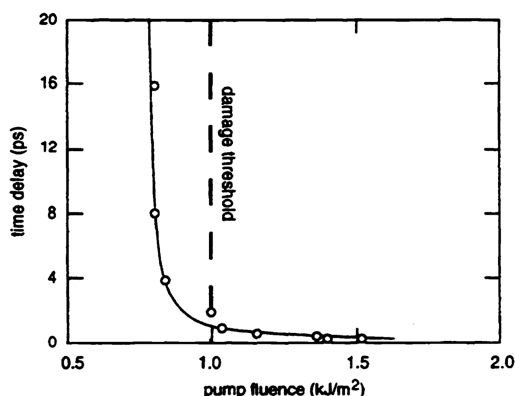


**Fig. 2 Pump-probe time delays at which Im[$\varepsilon$(2.2 eV)] is maximal and Re[$\varepsilon$(2.2 eV)] = 0 for different pump fluences. The solid curve is drawn to guide the eye.**

The dashed line in Fig. 2 at 1.0 kJ/m$^2$ indicates the threshold fluence for permanent damage to the sample. We determined this threshold by correlating pump pulse fluence with the size of damage spots on the sample measured through a microscope. Above the damage threshold the pump pulse induces irreversible changes in the sample while below the damage threshold the induced changes are reversible. Measurements taken several seconds after the excitation confirm that the dielectric constant eventually returns to its initial value for fluences below the damage threshold. Note that the absorption peak comes into resonance with the probe frequency even for pump fluences below the damage threshold.

## 3.1 Dielectric constant at 4.4 eV

We also measured the behavior of the dielectric constant at 4.4 eV under identical excitation conditions as in the 2.2 eV experiment. A summary of the data at 4.4 eV appears in Fig. 3. Figure 3a presents the time-dependence of the dielectric constant at 4.4 eV at the same four pump fluences shown in Fig. 1a while Fig. 3b is the 4.4-eV analogue to Fig. 1b. The dielectric constant in Fig. 3 exhibits behavior that is qualitatively similar to that in Fig. 1. Note, however, that the peak in Im($\varepsilon$) and the zero-crossing in Re($\varepsilon$) occur at earlier time delays in the 4.4-eV case than in the 2.2-eV case for equal pump fluence. Correspondingly, these features occur at lower fluences in Fig. 3b than in Fig. 1b for equivalent time delays. Re($\varepsilon$) at 4.4 eV crosses zero for fluences as low as 0.5 kJ/m$^2$ compared to the minimum fluence of 0.8 kJ/m$^2$ required for a zero-crossing at 2.2 eV. Furthermore, Im($\varepsilon$) at 4.4-eV does not rise far above its initial value of about 18 before dropping. At 4.4 eV the peak value of Im($\varepsilon$) is roughly three times smaller than the peak value at 2.2 eV.

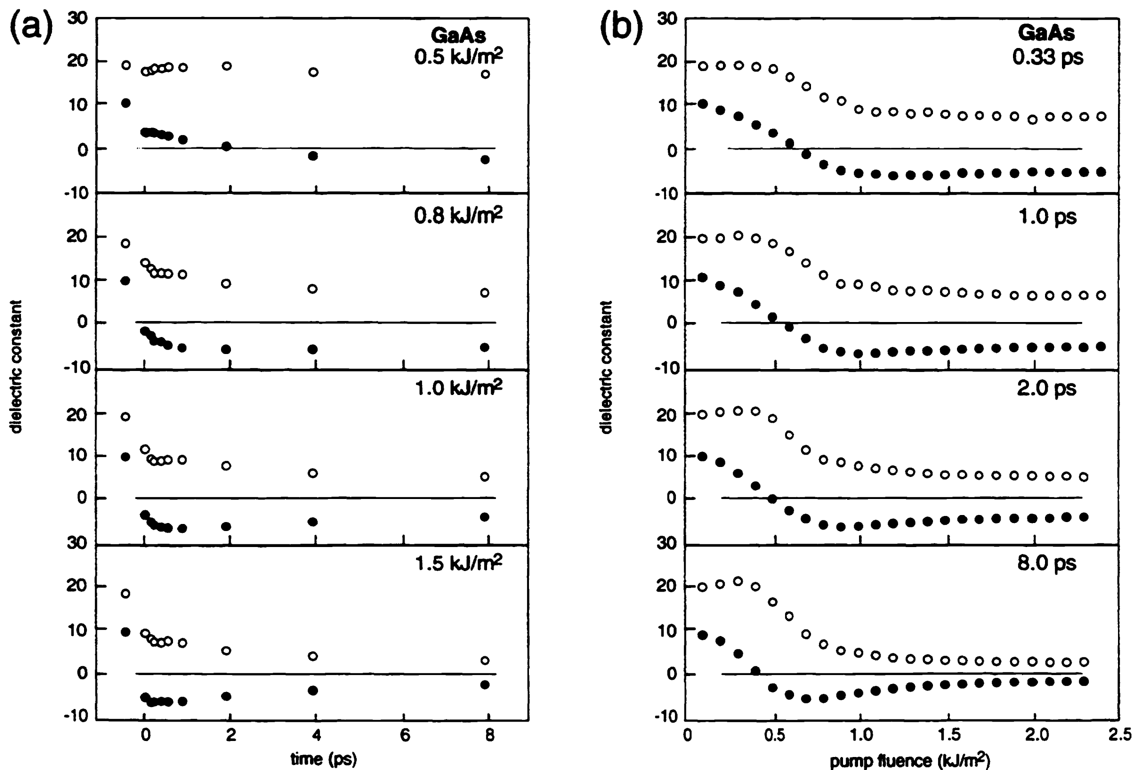


Fig. 3 a) Dielectric constant at 4.4 eV vs. pump-probe time delay for four different pump fluences. b) Dielectric constant at 4.4 eV vs. pump fluence for four different pump-probe time delays. ●: Re($\varepsilon$), ○: Im ($\varepsilon$).

## 4. Discussion

### 4.1 Band-gap collapse

The behavior of the dielectric constant at 4.4 eV is consistent with the picture of a drop in the resonant frequency of an absorption peak described in Section 3.1. The small rise in Im($\varepsilon$) at 4.4-eV indicates that this peak initially lies at a photon energy just above 4.4 eV. Following the pump pulse excitation, the center of the peak drops first through 4.4-eV and then continues down through 2.2-eV. A stronger excitation causes a faster drop through both probe frequencies. At pump fluences between 0.5 kJ/m$^2$ and 0.8 kJ/m$^2$, the excitation is strong enough to bring the resonant frequency of the absorption peak below 4.4 eV but not all the way down to 2.2 eV.

The plot of the dielectric function of GaAs shown in Fig. 4[14] lends support to this interpretation of our data. This plot shows the dielectric function in the absence of any excitation plotted vs. photon energy and corresponds to the initial state of the material in our experiments. The point $E_0$ at 1.4 eV marks the fundamental band edge below which Im($\varepsilon$) is zero; $E_1$ and $E_2$, located at 3.0 eV and 4.75 eV respectively,[15] label the two main absorption peaks in GaAs. These peaks arise from regions in the band structure in which the valence band is roughly parallel to the conduction band, resulting in a large joint density of states for direct interband transitions.[16] The $E_2$ peak, coincident with the zero-crossing in Re($\varepsilon$), is the stronger of the two absorption peaks, and its location approximately gives the value of the average bonding-antibonding splitting of GaAs.[17] Note that the location of the $E_2$ peak in the initial state does indeed lie just above the 4.4 eV probe photon energy.

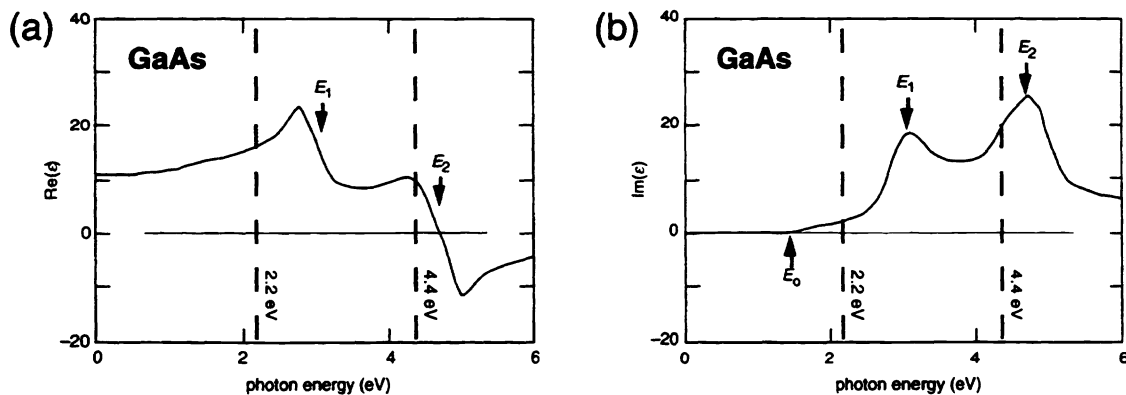


Fig. 2 a) Re($\varepsilon$) and b) Im ($\varepsilon$) for GaAs as a function of photon energy in the absence of any excitation.[14] $E_0$ corresponds to the minimum band gap, below which there is no absorption, while $E_1$ and $E_2$ label the two main absorption peaks.

At a fixed probe photon energy, a downward shift in the main absorption resonances in Fig. 4 results in the dielectric constant behavior we observe in our 2.2-eV and 4.4-eV data. As this shift begins to occur, Re($\varepsilon$) at 4.4 eV quickly drops through zero and Im($\varepsilon$) rises slightly to a peak before falling. As the shift

continues to lower photon energies, Im($\varepsilon$) at 2.2 eV, initially very small, rises by more than an order of magnitude. Meanwhile, Re($\varepsilon$) at 2.2 eV also rises somewhat before dropping sharply through zero as Im($\varepsilon$) reaches its peak.

In terms of the electronic band structure, a downward shift in the absorption peaks in the dielectric function results from a decrease in the average separation between the valence band and the conduction band. The data indicate that the average band gap drops from an initial value of 4.75 eV to below 2.2 eV for fluences above the damage threshold. If the *average* band gap drops by this much, the *minimum* band gap, initially at 1.4 eV, most likely drops to zero, suggesting that the pump pulse excitation induces a semiconductor-metal transition. The dielectric constant at high fluences and long time delays, after the collapse of the bandgap, is consistent with the characteristics of a poor metal and is similar to that of liquid carbon produced by femtosecond laser excitation.[18]

The striking resonance behavior we observe indicates that the response of the dielectric constant to the excitation is dominated by changes in the electronic band structure rather than by free carrier contributions to the optical susceptibility. One can get a sense for the size of the direct free carrier effects by looking at low fluence data where the band structure changes are not strong enough to overwhelm the free carrier contributions. At 0.5 kJ/m$^2$, for example, Re($\varepsilon$) at 2.2 eV shows an almost instantaneous decrease followed by a slower recovery. At this fluence, which is significantly below the damage threshold, the band structure changes are relatively small and should lead to a slight increase in Re($\varepsilon$) based on the slope of the dielectric function vs. photon energy at 2.2 eV. The initial decrease results from the Drude term contribution of the excited free carriers, which is stronger at 2.2 eV than at 4.4 eV because of the approximately $1/\omega^2$ dependence of the Drude term. As the free carrier population decreases due to strong Auger recombination, the Drude term contribution decreases and Re($\varepsilon$) recovers. The observed recovery time of a few picoseconds agrees with the predicted high-density Auger recombination time.[19] At fluences high enough to induce a collapse of the band gap, however, the band structure resonance behavior is so strong that it masks the Drude term contributions to the dielectric constant.

## 4.2 Electronic screening and structural change

The data presented in this paper conclusively show that the femtosecond laser pulse excitation leads to a major change in the electronic band structure marked by the drop in the average separation between the valence band and the conduction band. What underlying physical effects are responsible for this alteration? To answer this question, we should examine two main sources of band structure modification: electronic screening and structural change.

Through electron-hole pair generation, the pump pulse creates a large population of mobile charge carriers that can partially screen the ionic potential in the material. In screening this potential, the charge carriers reduce the average bonding-antibonding splitting, corresponding to a decrease in the average separation between the valence and conduction bands. A recent calculation shows

that when 10% of the valence electrons are excited to the conduction band, the direct gap at the X-point in the band structure of GaAs will decrease by roughly 2 eV due to electronic screening and many-body band gap renormalization.[20] Note that this effect, in which the free carriers instantaneously affect interband transitions by modifying the band structure, is different from the direct intraband contribution of the free carriers to the dielectric constant through a Drude term and may play a significant role in the changes to the dielectric constant at early time delays. However, as in the case of the Drude contributions, the effect of electronic screening on the dielectric constant should be largest when the free carrier density is highest — *i.e.* immediately following the excitation. As Auger recombination and diffusion reduce the free carrier density, the dielectric constant should recover towards its initial value within a few picoseconds. But the data show that the change in the dielectric constant *increases* with time delay during the picoseconds following the excitation. Electronic screening by itself, therefore, cannot explain the data.

To account for the time evolution of the dielectric constant, we must examine the effect of lattice structural change on the band structure. The electronic band structure is fundamentally intertwined with the crystal structure. The semiconducting behavior of Group IV and III-V materials such as GaAs arises from the tetragonally-coordinated diamond or zincblende arrangement of the constituent atoms. If this arrangement is disturbed, the electronic properties will change accordingly. In general, deformation of the diamond or zincblende structure leads to a collapse of the band gap and a semiconductor-metal transition.[17,21-23] Even a 10% change in average bond length is enough to cause a semiconductor-metal transition.[23] Note that an ionic velocity as small as 25 m/s is sufficient to achieve a 10% change in the GaAs bond length within 1 ps.

Because the covalent bonds of semiconductors like GaAs are stabilized by the valence electrons, excitation of a sufficient number of electrons from bonding valence states to antibonding conduction states can lead directly to lattice instability.[2,24,25] If the femtosecond pump pulse is intense enough to excite this critical density of electrons, the resulting instability in the lattice will cause the atoms to deform towards a new minimum potential energy configuration. This deformation begins immediately following the excitation but continues to evolve for several picoseconds after it. The change in the dielectric constant accompanying the lattice deformation will therefore also continue to progress in the picoseconds following the excitation, in agreement with the observed behavior of the dielectric constant.

## 5. CONCLUSION

Our data show that a Drude model cannot be used to analyze high-intensity femtosecond pump-probe reflectivity measurements. At pump fluences on the order of the damage threshold, the excitation causes major changes in the electronic band structure. Because of these changes, the behavior of $\chi(\omega)_{\text{interband}}$ rather than $\chi(\omega)_{\text{Drude}}$ dominates the response of the dielectric constant to the excitation.

The femtosecond laser pulse excitation induces a drop in the average separation between the valence band and the conduction band. This drop manifests itself in a decrease of the main absorption resonances in the GaAs dielectric function. The rate and extent of the drop in average valence-conduction band separation increases with pump fluence. For high enough fluence, the zero-crossing in Re($\varepsilon$) falls from an initial value of 4.75 eV to below 2.2 eV, indicating a collapse in the band structure. While electronic screening may account for a significant amount of the initial drop in resonant frequency, the continuation of this drop for picoseconds following the excitation most likely results from lattice deformation caused by destabilization of the covalent bonds.

## ACKNOWLEDGMENTS

We appreciate many useful discussion with Professors N. Bloembergen, H. Ehrenreich, and E. Kaxiras. E. Glezer gratefully acknowledges a Fannie and John Hertz Fellowship. This work was supported by contract numbers ONR N00014-89-J-1023 and NSF DMR 89-20490.

## REFERENCES

1. E. I. Shtyrkov, I. B. Khaibullin, M. M. Zaripov, M. F. Galyatudinov, and R. M. Bayazitov, "Local laser annealing of implantation doped semiconductor layers," *Sov Phys-Semicond* **9**, 1309, 1976.
2. J. A. Van Vechten, R. Tsu, and F. W. Saris, "Nonthermal pulsed laser annealing of Si; plasma annealing," *Phys. Lett.* **74A**, 422, 1979.
3. J. A. Kash, J. C. Tsang, and J. M. Hvam, "Subpicosecond time-resolved Raman spectroscopy of LO phonons in GaAs," *Phys. Rev. Lett.* **54**, 2151, 1985.
4. H. W. K. Tom, G. D. Aumiller, and C. H. Brito-Cruz, "Time-resolved study of laser-induced disorder of Si surfaces," *Phys. Rev. Lett.* **60**, 1438, 1988.
5. S. V. Govorkov, I. L. Shumay, W. Rudolph, and T. Schroeder, "Time-resolved second-harmonic study of femtosecond laser-induced disordering of GaAs surfaces," *Opt Lett* **16**, 1013, 1991.
6. K. Sokolowski-Tinten, H. Schulz, J. Bialkowski, and D. von der Linde, "Two distinct transitions in ultrafast solid-liquid phase transformations of GaAs," *Appl Phys A* **53**, 227, 1991.
7. P. N. Saeta, J. Wang, Y. Siegal, N. Bloembergen, and E. Mazur, "Ultrafast electronic disordering during femtosecond laser melting of GaAs," *Phys. Rev. Lett.* **67**, 1023, 1991.
8. C. V. Shank, R. Yen, and C. Hirlimann, "Time-resolved reflectivity measurements of femtosecond-optical-pulse-induced phase transitions in Silicon," *Phys Rev Lett* **50**, 454, 1983.
9. H. Kurz, and N. Bloembergen, "Picosecond Photon-Solid Interaction," *Energy Beam-Solid Interactions and Transient Thermal Processing*, eds. D. K. Biegelsen, G. A. Rozgonyi, and C. V. Shank, 3, Materials Research Society, Pittsburgh, 1985.
10. H. M. van Driel, "Kinetics of high-density plasmas generated in Si by 1.06- and 0.53-μm picosecond laser pulses," *Phys Rev B* **35**, 8166, 1987.

11. J. K. Wang, Y. Siegal, C. Z. Lü, and E. Mazur, "Generation of dual-wavelength, synchronized, tunable, high energy, femtosecond laser pulses with nearly perfect Gaussian spatial profile," *Opt. Comm.* **91**, 77, 1992.

12. D. L. Greenaway, and G. Harbeke, *Optical Properties and Band Structure of Semiconductors*, Pergamon Press, Oxford, 1968.

13. R. F. Potter, "Pseudo-Brewster Angle Technique for Determining Optical Constants," *Optical Properties of Solids*, eds. S. Nudelman, and S. S. Mitra, Chapter 16, Plenum Press, New York, 1969.

14. E. D. Palik, "Gallium Arsenide," *Handbook of Optical Constants of Solids*, eds. E. D. Palik, 434, Academic Press, Inc., New York, 1985.

15. D. E. Aspnes, G. P. Schwartz, G. J. Gualtieri, A. A. Studna, and B. Schwartz, "Optical properties of GaAs and its electrochemically grown anodic oxide from 1.5 to 6.0 eV," *J. Electrochem. Soc.* **128**, 590, 1981.

16. M. L. Cohen, and J. R. Chelikowsky, *Electronic Structure and Optical Properties of Semiconductors*, Springer-Verlag, Berlin, 1988.

17. W. A. Harrison, *Electronic Structure and the Properties of Solids: The Physics of the Chemical Bond*, Dover, New York, 1989.

18. D. H. Reitze, H. Ahn, and M. C. Downer, "Optical properties of liquid carbon measured by femtosecond spectroscopy," *Phys Rev B* **45**, 2677, 1992.

19. E. J. Yoffa, "Dynamics of dense laser-induced plasmas," *Phys. Rev. B* **21**, 2415, 1980.

20. D. Kim, H. Ehrenreich, and P. Young, "Band structure of femtosecond-laser-pulse excited GaAs," *Solid State Comm.*, accepted for publication.

21. V. M. Glazov, S. N. Chizhevskaya, and N. N. Glagoleva, *Liquid Semiconductors*, Plenum Press, New York, 1969.

22. W. Jank, and J. Hafner, "Electronic Structure of Molten Si, Ge, and GaAs," *J. Non-Crystalline Solids* **114**, 16, 1989.

23. S. Froyen, and M. L. Cohen, "Structural properties of III-V zinc-blende semiconductors under pressure," *Phys. Rev. B* **28**, 3258, 1983.

24. R. Biswas, and V. Ambegoakar, "Phonon spectrum of a model of electronically excited silicon," *Phys. Rev. B* **26**, 1980, 1982.

25. P. Stampfli, and K. H. Bennemann, "Theory for the instability of the diamond structure of Si, Ge, and C induced by a dense electron-hole plasma," *Phys. Rev. B* **42**, 7163, 1990.